SAND2010-8719P

Kull Magnetic Physics Overview

Thomas A. Gardiner

Sandia National Laboratories

December 15, 2010

Sandia National Laboratories is a multi-program laboratory managed and operated by Sandia Corporation, a wholly owned subsidiary of Lockheed Martin Corporation, for the U.S. Department of Energy's National Nuclear Security Administration under contract DE-AC04-94AL85000.

The Start of Kull Magnetics

- Kull is an ASC HEDP code, originally developed at LLNL.
- In 2007 an MOU was signed making Kull jointly owned by LLNL and SNL.
- In 2008 we began developing in earnest the Magnetic Physics capabilities in Kull.
- The key challenge is to develop these capabilities in a manner which is interoperable with the existing algorithms.
  - Kull uses the (Caramana, Burton, Shashkov, Whalen) compatible hydrodynamics algorithm.
  - Kull supports arbitrary polygonal / polyhedral mesh elements.
- For Z-pinch applications Kull must be stable at LOW β.

The Talk Overview

- Spatial Discretization (Lagrangian Ideal MHD)
  - Satisfying $\nabla \cdot \mathbf{B} = 0$
  - Supporting arbitrary mesh elements
  - Hourglass stability
  - Successful Initial Tests
- Circuit Coupled Resistive Diffusion
- Magnetic Field Remap
- *B*-field Reconstruction & second order corrections
- Integrated tests

Compatible Hydro. Hourglass Stability

- Consider 4 quads, arrows showing nodal motion
- The CBSW compatible hydro. is stable for hourglass modes.
- Stability is derived from sub-zonal corner pressure corrections.
- Pressure corrections are derived from corner masses.

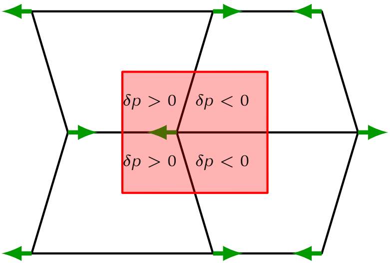

The hydrodynamics uses subzonal corner pressures.

MHD Hourglass Stability

- Normal magnetic flux discretized on side faces.
- Flux is constant during Lagrange step.
- Physics based hourglass control (no knobs).
- Nodal force via Maxwell stress integral.

$$\mathbf{F} = \oint \left[\frac{\mathbf{B} \otimes \mathbf{B}}{\mu_0} - \frac{|\mathbf{B}|^2}{2\mu_0} \right] \cdot d\mathbf{A}$$

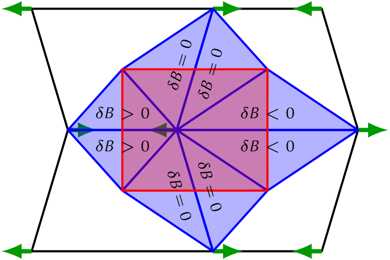

The MHD uses subzonal side magnetic fields.

Side Magnetic Field Mesh Elements

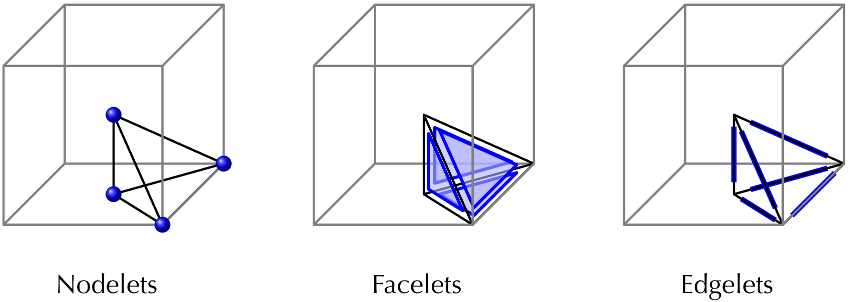

- Extended KULL's infrastructure to support new elements.
- Many more unknowns: 5 NL/N, 10 EL/E, 8 FL/F, 30 EL/Z
- Our method supports arbitrary polyhedrons, not just hexes.

Low β MHD Equilibrium

- The ideal MHD equilibrium is described by the Grad-Shafranov equation.

$$\nabla^2 \psi = -\mu \left(\frac{dP}{d\psi} \right) \quad \text{where} \quad \mathbf{B}_p = \nabla \psi \times \hat{\mathbf{k}}$$

$$P(\psi) = 10^{-8} + 2 \left(\frac{\psi}{\psi_{max}} \right)^2 \quad \text{with} \quad \psi = 0 \quad \text{B. C.'s}$$

- We solve this equation using relaxation giving ψ on nodelets.
- From ψ we initialize magnetic flux on facelets in Kull.
- Average $P(\psi)$ on nodelets to get zone-average P.
- Due to averaging the pressure, and stress discretization differences, the initial state in Kull is a perturbed equilibrium.

Robust Low β MHD Equilibrium

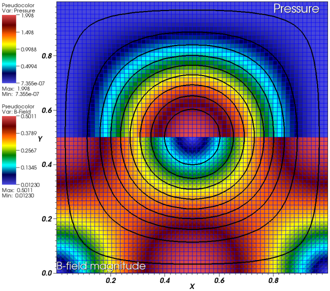

P and $|\mathbf{B}|$ in Grad-Shafranov problem.

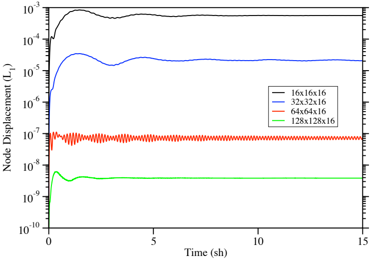

Maximum node displacement converges toward zero.

- 2D equilibria in 2D or 3D domain are accurately simulated.
- $\beta = P_{\text{hydro}}/P_{\text{mag}} \approx 10^{-7}$ near boundary.

MHD Blast Wave

- High pressure ($P = 10$) region in a low pressure ($P = 0.1$) ambient.
- Embed a uniform magnetic field ($B^2/2\mu = 0.5$)
- Plasma $\beta = (20, 0.2)$ inside, outside
- Initially uniform density
- Similar to Sedov, but...

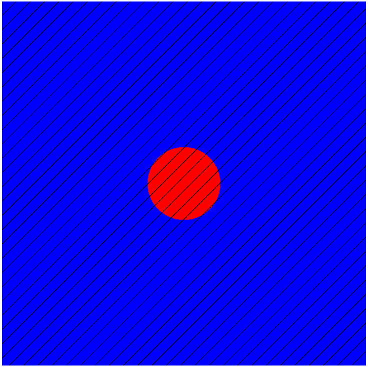

Pressure and Magnetic Field Lines

MHD Blast Wave is Robust

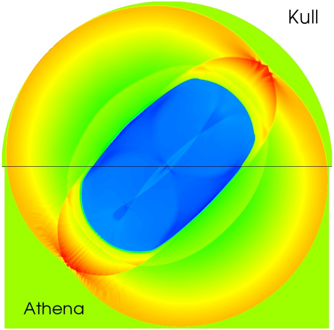

Log Density

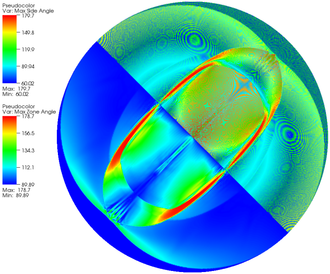

Maximum mesh angle (zone and side) $\approx 180°$.

- Lagrangian KULL is compared to Eulerian Godunov Athena.
  - Complex shock / contact boundaries lines up.
  - Both codes show slow-mode corrugation instability.
  - Lagrangian Kull is stable at large mesh angles.

Magnetic Diffusion Solves Ohm's Law

$$\nabla \times \frac{\Delta t}{\mu_0} \nabla \times \mathbf{E}^{n+1} + \overline{\overline{\sigma}} \cdot \mathbf{E}^{n+1} = \nabla \times \frac{\mathbf{B}^n}{\mu_0}$$

Discretize **E** with edge finite elements:

$$\mathbf{E} = \sum_e E_e \mathbf{w}^e$$

$$\mathbf{B}^{n+1} = \mathbf{B}^n - \Delta t \nabla \times \mathbf{E}^{n+1}$$

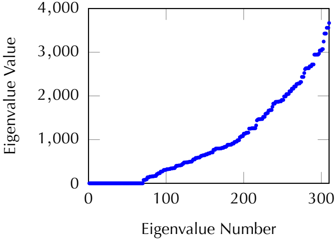

- This equation for the current is (nearly) singular
- In pure void, $\sigma = 0$ and $\mathbf{J} = \sigma \mathbf{E} = 0$, so **E** unconstrained
- Use CG with *hypre*'s Auxiliary-space Maxwell Solver as preconditioner
  - Solves two, easier, nodal problems and projects to edge
  - In void, we add the constraint $\mathbf{E} = \nabla \phi$ to make it non-singular
- Using pure void is more robust than using a small σ
  - A small conductivity is resolution dependent: $\sigma_{\text{small}} \sim 1/\Delta x$
  - Extra work for void is about 10% slower than using a floor

Magnetic Diffusion can be driven by an external circuit

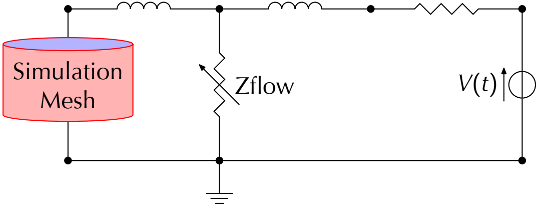

- Use an equivalent circuit for the Z-machine to drive the simulation load.
- Reused ALEGRA circuit code. (Thanks Tom Haill.)
- Circuit model uses IDA from Sundials.
- Total electric field is sum of two others: $\mathbf{E} = \mathbf{E}_0 + I\mathbf{E}_1$.
    - This means two linear solves to get parameters that are passed to circuit solver.
    - Circuit solver returns current and voltage across mesh, and we finalize solution.

Cost of robustness and generality is unknowns

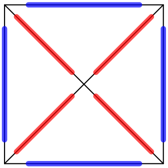

6 vs. 2 edges/zone (RZ)

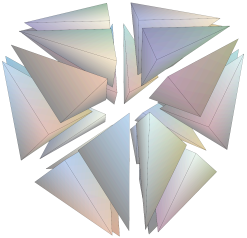

Each hex has 24 tets

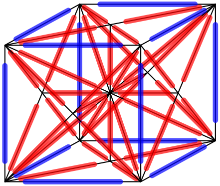

29 vs. 3 edges/zone (3D)

- Relative to a standard quad or hex discretization (in blue)
  - In 2D-XY, we have twice the unknowns
  - In 2D-RZ, we have thrice the unknowns
  - In 3D, we have 10 times the unknowns

What if we can eliminate some unknowns before *hypre* sees the matrix?

During matrix assembly, we eliminate unknowns

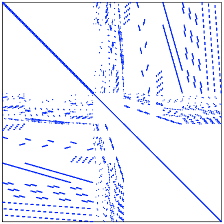

Total 3D matrix **A**

- Full matrix is sum of tet matrices

$$\mathbf{A} = \sum_t \mathbf{A}_t$$

- We form groups of tets into clumps

$$\mathbf{A} = \sum_c \mathbf{A}_c \quad \text{with} \quad \mathbf{A}_c = \sum_{t_g} \mathbf{A}_{t_g}$$

- Edges are interior to the clump or on the boundary

$$\mathbf{A}_c \mathbf{x}_c = \mathbf{y}_c \quad \rightarrow \quad \begin{bmatrix} \mathbf{A}_{ii} & \mathbf{A}_{ib} \\ \mathbf{A}_{bi} & \mathbf{A}_{bb} \end{bmatrix} \begin{bmatrix} \mathbf{x}_i \\ \mathbf{x}_b \end{bmatrix} = \begin{bmatrix} \mathbf{y}_i \\ \mathbf{y}_b \end{bmatrix}$$

- Interior edges are eliminated with Schur complement

$$\left(\mathbf{A}_{bb} - \mathbf{A}_{bi}\mathbf{A}_{ii}^{-1}\mathbf{A}_{ib}\right)\mathbf{x}_b = \mathbf{y}_b - \mathbf{A}_{bi}\mathbf{A}_{ii}^{-1}\mathbf{y}_i \quad \rightarrow \quad \mathbf{A}_r \mathbf{x}_b = \mathbf{y}_r$$

- What tets do we choose when making clumps?

Sandia National Laboratories

In 2D we eliminate the zone-interior unknowns

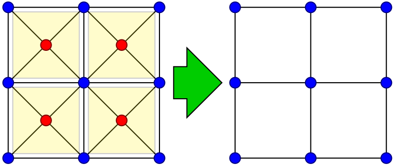

Reduce XY to node mesh

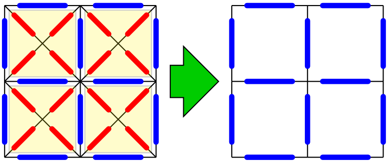

Reduce RZ to edge mesh

Mesh Type	rows/quad	matrix entries/quad	matrix entries/row
XY original	2	14	7
XY quad	1	9	9
RZ original	6	30	5
RZ quad	2	14	7

- Number of unknowns and matrix entries are lower.
  - But matrix is less sparse
- We have recovered the same number of unknowns and nonzeros as the standard quad discretizations
  - But the discretization is not the same

In 3D we must think outside the box

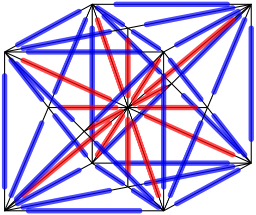

The tetrakis hexahedron is the obvious clump of tets

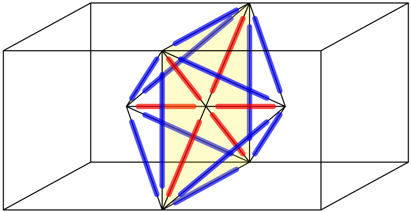

The octahedron that spans each face is a much better clump of tets

- Reduction increases matrix bandwidth
- Good performance tied more to matrix size than unknowns

Mesh Type	rows/hex	matrix entries/hex	matrix entries/row
"tet'd" hex (original)	29	461	16
tetrakis hexahedron	15	1107	74
octahedron	11	335	30
standard hex	3	99	33

A tetrakis hexahedron is a non-regular icositetrahedron (24-sided polyhedron) formed by adding square pyramids to the faces of a hexahedron.
Eric W. Weisstein, *Mathworld*, `http://mathworld.wolfram.com/TetrakisHexahedron.html`

The reduced matrix has nice mathematical properties

- Many of the original matrix properties carry over to the reduced matrix
  - The reduced matrix is sparse, unlike most Schur complements
  - The AMS preconditioner works on the reduced matrix
  - In 2D the reduced matrix has the same graph as a standard quad discretization
- Some properties are much better for the reduced matrix
  - The condition number is lower
  - The ratio between the strongest and weakest off-diagonals in the matrix is better, making it easier for AMS/AMG to make good choices about eliminating entries
  - In 2D the reduced matrix is even nicer than the standard quad discretization
- It is as if we discretized directly on the reduced mesh
  - But we get solutions for all of the original unknowns.

See Brunner and Kolev, "Alegraic multigrid for linear systems obtained by explicit element reduction," submitted to *SIAM Journal on Scientific Computing*, July 2010

Conductivity jump and varying aspect ratio

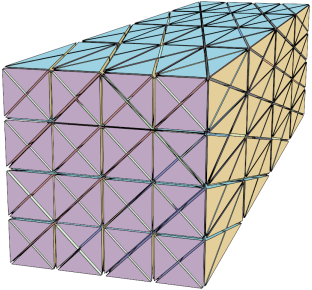

The mesh in the 3D problem

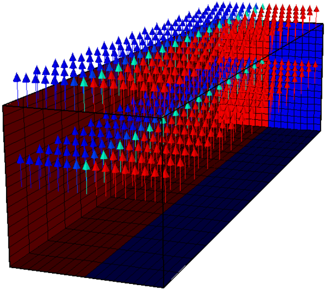

B-field (arrows) and conductor (red)

- A magnetic field diffuses from a void region into material
- The mesh is stretched to create zones with high aspect ratios, keeping resolution in the interesting direction fixed
- We compare run times and iteration counts for 2D-XY, 2D-RZ, and 3D-XYZ geometries

Speed-up improves as aspect ratio increases

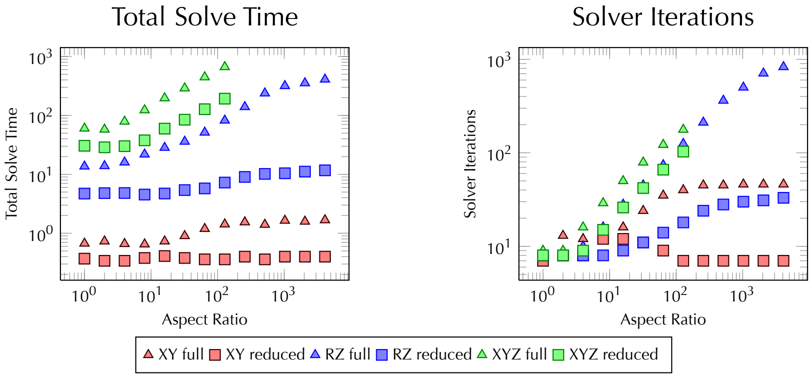

- Solve times are always faster with the reduced matrix
    - XY: 1.7-4.2× , XYZ: 2.0-3.5×, RZ: 2.9-35×!
- Speed-up from smaller matrix and reduced iteration count
- Setup is faster, despite extra work

Comparison of hex-only to sub-tet'd discretizations

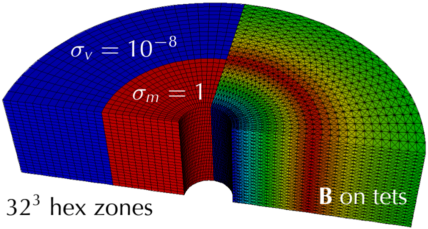

- Run the same problem multiple ways
  - Kull: tet'd hex
  - Kull: reduced matrix
  - Ares: pure hex
- Both Kull methods solve same system
- *hypre* used to solve both

Mesh	rows	matrix entries	code setup	*hypre* solve	total time	iters
Tet (K)	969k	15.2M	18.5	107.0	125.5	13
Reduced (K)	367k	10.9M	12.9	33.5	46.4	9
Hex (A)	105k	3.3M	5.9	16.4	22.3	18
Ratio (K/A)	*9.3*	*4.6*	*2.2*	*2.0*	*2.1*	*0.5*

- Kull runtime $2\times$ slower for $9.3\times$ more unknowns
  - Need to run convergence study, plotting error vs. runtime
- Condition number improves from hex to tet to reduced

Magnetic Field Remap Overview

- Given a discrete solution ($\phi_i = \int_{\Omega_i} \mathbf{B} \cdot d\mathbf{S}$) on an initial (old) mesh, determine the solution on a final (new) mesh.
- Overlay Method:
  1. Realize the discrete solution on the old mesh $\phi_i \rightarrow \mathbf{B}(\mathbf{x})$.
  2. Compute the ϕ_i on the new mesh as an integral average.
- Advection Method:
  1. Consider the old and new mesh as connected by advection from time states t^n and t^{n+1}.
  2. Use Galilean invariance to transform problem to one of the magnetic field moving through the mesh.
  3. Solve the remap problem as an advection problem.
- Analytically these methods are identical - not necessarily true numerically.
- Consequently, advection methods are CFL stability limited.

Requirements & Solution Method

- Triangle / Tetrahedron mesh is refined relative to Zone mesh.
- Therefore, remap must be accurate & stable for CFL > 1.
- Remap must preserve $\nabla \cdot \mathbf{B} = 0$ identically.
- Remap should be a local explicit operator.
- Solution: Use a vector potential to compute EMF.
  - Consistent Overlay and Advection method.
  - No CFL stability limit.
  - Parallel synchronization of EMF ensures $\nabla \cdot \mathbf{B} = 0$.

Advection Method

- A mesh nodelet is displaced by a distance $\mathbf{d}$.
- Consider this to occur over a time step $\delta t = t^{n+1} - t^n$ with a constant velocity $\mathbf{v} = \mathbf{d}/\delta t$.
- Galilean invariance – the field moves through the mesh with a velocity $\mathbf{v}_g = -\mathbf{d}/\delta t$.
- Remap is governed by Faraday's law for an ideal fluid

$$\frac{\partial \mathbf{B}}{\partial t} + \nabla \times \mathbf{E} = 0$$

where $\mathbf{E} = \mathbf{B} \times \mathbf{v}_g$.

Computing the CT EMF

- Constrained Transport integral relations depend on the "time" and edge integrated electric fields.

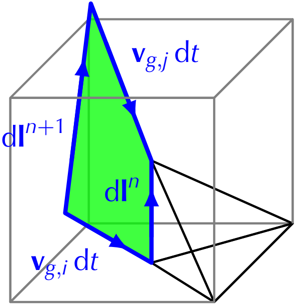

$$\int_{t^n}^{t^{n+1}} \int \mathbf{E}\cdot \mathrm{d}\mathbf{l}\,\mathrm{d}t = \int_{t^n}^{t^{n+1}} \int (\mathbf{B}\times \mathbf{v}_g)\cdot \mathrm{d}\mathbf{l}\,\mathrm{d}t$$
$$= \int_{t^n}^{t^{n+1}} \int \mathbf{B}\cdot (\mathbf{v}_g\,\mathrm{d}t \times \mathrm{d}\mathbf{l})$$
$$= \oint \mathbf{A}\cdot \mathrm{d}\mathbf{l}'$$

- Note that the result is gauge invariant.
- The gauge need not be parallel consistent.

Multipolar / Poincaré Gauge

- This gauge is distinguished by its local gauge condition.

$$\mathbf{A}_m(\mathbf{x},t)\cdot\mathbf{x}=0$$

- From this one can construct an integral relation

$$\mathbf{A}_m(\mathbf{x},t)=-\mathbf{x}\times\int_0^1 u\mathbf{B}(u\mathbf{x},t)\,\mathrm{d}u$$

- It proves the existence of a local solution and is a generalization of $\mathbf{A}=\frac{1}{2}\mathbf{B}\times\mathbf{x}$.
- $\mathbf{A}$ is integrated outward in a breadth before depth manner.

Field Loop Advection

- The magnetic field is initialized as $\mathbf{B} = B_0 \hat{e}_\theta$.
- The current density is singular at the center and boundary.
- The magnetic field is advected in a Lissajous figure (figure 8) using the remap operator.
- Every 100 cycles the B-field returns to the initial position.
- Results for a linear reconstruction and MCD limiter shown on right.

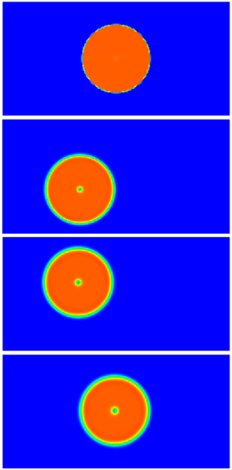

Magnitude of B

Field Loop Energy Evolution

- The Constant B case looses $\sim 30\%$ energy after 100 cycles.
- The Linear B (MCD) case looses $\sim 5\%$ energy after 100 cycles.

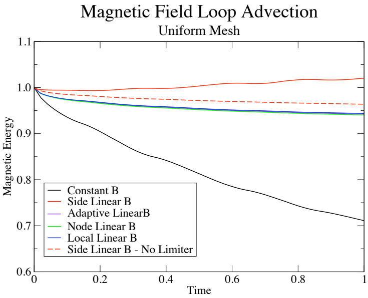

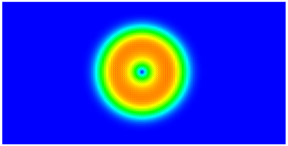

Constant B

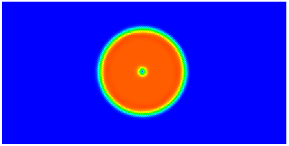

Linear B

Field Loop Remap is Insensitive to Mesh

- Mesh is randomly distorted by moving nodes up to 30% of zone size.
- Magnetic energy evolution is identical to eye norm.

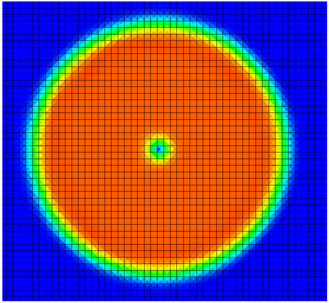

Uniform Mesh

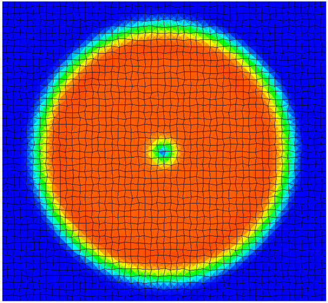

Random Mesh

Magnetic Field Convergence

- I developed a variety of reconstruction alg.
- All recover a linear B-field exactly on an arbitrary (random) mesh.
- The magnetic field at side-center converges at order 2.
- The magnetic field is sinusoidal:

$$B_x = -\cos(kx)\sin(ky)$$
$$B_y = \sin(kx)\cos(ky)$$

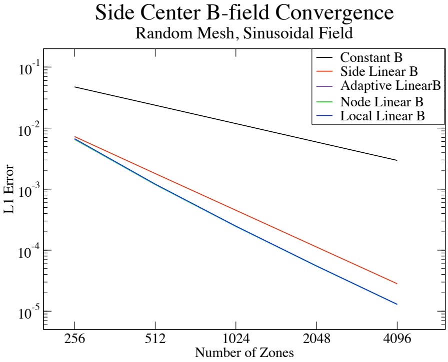

Maxwell Stress Convergence

- The nodal force is exact for linear **B**.
- The nodal force converges at order 2 on a sinusoidal mesh.
- The nodal force converges at order 1.2 on a random mesh. (measurement error?)

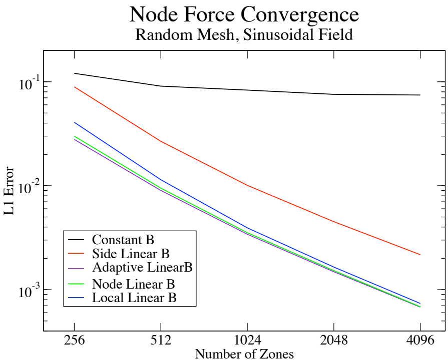

Thin Shell Imploding Liner

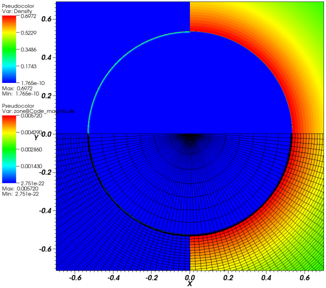

A thin cylindrical shell is imploded.

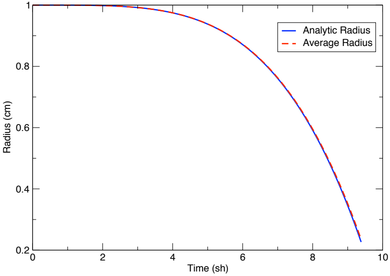

We agree well with analytic model

- Analytic, self-similar, thin shell implosion model (Slutz et al., Phys. Plasmas, v. 8, p. 1673 (2001)
- Useful test in (x, y)-, (r, z)- and (x, y, z)-geometries
- In (x, y, z)-geometry weakly dependent on angular resolution, $\sim$ 10 angular zones is sufficient.
- Either circuit or H-tangent boundary conditions

MRT Unstable Imploding Liner

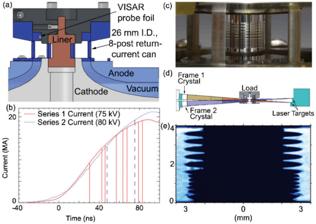

Perturbed Al liner seeds MRT growth.

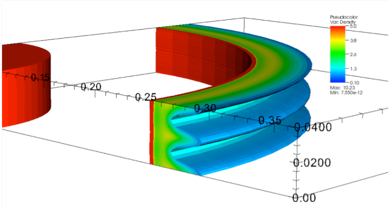

3D MRT simulation at time = 75.5 ns.

- Measurements of Magneto-Rayleigh-Taylor Instability… (Sinars et al., Phys. Rev. Letters, v. 105, p. 185001 (2010)
- 25 & 400 μm sinusiodal perturbations seed the instability.
- 15 μm resolution radiographs capture liner outer surface evolution.
- Multiple images enable simulation verification.

Summary

- Kull is a LLNL / SNL jointly owned ASC HEDP code
- We are developing the MHD capabilities to be consistent with the CBSW compatible hydro. scheme.
- Lagrangian calculations demonstrate a robust algorithm using a compatible **B**-field discretization on a triangle / tetrahedron sub-grid.
- Circuit coupled resistive diffusion is accelerated using a Schur complement.
- Magnetic Field Remap uses a consistent advection / overlay method via a vector potential.
- Limited **B**-field reconstruction resolves linear variation on an arbitrary (random) mesh exactly. Generally second order convergence...
- Magneto-Rayleigh-Taylor validation effort is underway.

MHD Blast Wave
Slow-mode Shock Corrugation Instability

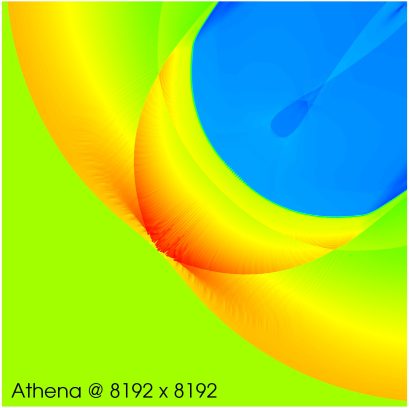

Log Density